NUCL SCI TECH (2019) 30:116
https://doi.org/10.1007/s41365-019-0634-y

Analyzing the transient effects of ^{60}Co gamma rays in a CIS by Monte Carlo method

Yuan-Yuan Xue[1] · Zu-Jun Wang[1] · Min-Bo Liu[1] · Rui Xu[2] · Hao Ning[2] · Wen Zhao[1] · Bao-Ping He[1] · Zhi-Bin Yao[1] · Jiang-Kun Sheng[1] · Wu-Ying Ma[1] · Guan-Tao Dong[1]

Received: 14 September 2018 / Revised: 19 February 2019 / Accepted: 20 March 2019 / Published online: 15 June 2019

Abstract The objective of this work is to analyze the transient effects of ^{60}Co gamma rays in the CMOS image sensor (CIS) using the Monte Carlo method, based on Geant4. The track, energy spectrum, and angle of produced electrons when gamma rays traversed a silicon or silicon dioxide cube were calculated. A simplified model of a 500 × 500 CIS array was established, and the transient effects of gamma rays in the CIS were simulated. The raw images were captured when the CIS was irradiated by gamma rays. The experimental results were compared with the simulation results. The characteristics of the typical events induced by transient effects were analyzed.

Keywords ^{60}Co gamma rays · Transient effects · CMOS image sensor (CIS) · Geant4

1 Introduction

The CMOS image sensor (CIS) [1, 2] is an attractive device for use in many scientific applications, such as star tracking, space remote sensing, and particle or ray track observation. When it is used in these harsh radiation environments, it can be damaged by particles or rays. The main radiation damage effects include the total ionizing dose (TID) effects, displacement damage dose (DDD) effects, and transient effects. As opposed to the transient effects, the TID and DDD effects are cumulative.

The TID and DDD effects on the CIS have been widely investigated. Hopkinson et al. [3, 4] presented proton, heavy ion, and gamma radiation effects on CISs. Goiffon et al. [5–7] conducted considerable work on the TID and DDD effects on CISs with different structures. Wang et al. [8–10] also investigated the TID and DDD effects on CISs at different dose rates. The degradation of dark current, dark signal non-uniformity, random noise, saturation output, signal-to-noise ratio, image lag, and charge transfer inefficiency versus the TID and DDD were presented. Wang et al. [2] and Cheng et al. [11] presented some interesting experimental results on the transient effects of gamma rays in CISs. There have been extensive studies on the radiation damage in CISs, but few studies have focused on the transient effects, especially using the Monte Carlo method.

The purpose of this study is to analyze the transient effects of ^{60}Co gamma rays in a CIS using the Monte Carlo method, based on Geant4 [12, 13]. Based on particle interactions, the primary physical processes of the interaction of gamma rays and silicon (Si) or silicon dioxide (SiO_2) were analyzed. The track, energy spectrum, and angle of produced electrons when gamma rays traversed

This work was supported by the National Natural Science Foundation of China (Nos. 11805155, 11875223, and 11690043), the Chinese Academy of Sciences strategic pilot science and technology project (No. XDA15015000), the Innovation Foundation of Radiation Application (No. KFZC2018040201), and the Foundation of State Key Laboratory of China (Nos. SKLIPR1803 and 1610).

✉ Zu-Jun Wang
wangzujun@nint.ac.cn

[1] The State Key Laboratory of Intense Pulsed Radiation Simulation and Effect, Northwest Institute of Nuclear Technology, Xi'an 710613, China

[2] School of Materials Science and Engineering, Xiangtan University, Xiangtan 411105, China

through a Si or SiO_2 cube were calculated. A three-dimensional structure of the CIS array was established. In addition, the transient effects of gamma rays in CIS were simulated. Gamma ray irradiation experiments were conducted in a laboratory at the Northwest Institute of Nuclear Technology. The dose rate was approximately 0.1 rad(Si)/s. The raw images were captured by our measurement system when the CIS was irradiated by gamma rays. The simulation and experimental results were compared with each other and may help us to understand the characteristics of the transient effects of ^{60}Co gamma rays in CISs.

2 Simulation details

In this work, the three-dimensional Monte Carlo code Geant4 version 10.0 is used to model the transient effects of ^{60}Co gamma rays in a CIS (see Fig. 1). Radiation effects induced by gamma rays in materials include photoelectric effects, Compton scattering, and pair effects. All of these effects have been adopted in the Geant4 simulation. When the gamma rays pass through the material, they collide with orbital electrons or pass near the nucleus and consequently cause radiation effects. The gamma rays can displace an orbital electron and give all of their energy to the electron through the photoelectric effects. Also, they could displace an orbital electron and give some of their energy to the electron through Compton scattering. Besides, when the kinetic energy of a photo of the gamma rays is more than 1.02 MeV and passes very close to the nucleus, the photon disappears and produces an electron pair (electron and positron) through the pair effect. The produced electron would lose its energy through the ionization process and produce electron holes surrounding the track, inducing transient effects in the CIS.

There are two γ-quanta generated at one radioactive decay of the ^{60}Co gamma ray source. The energy of the gamma-quanta is 1.33 or 1.17 MeV, with a mean value of 1.25 MeV [14].Therefore, the photoelectric effect, Compton scattering, and pair effect should be considered in physics simulations. When the ^{60}Co gamma rays pass through the CIS, there are many electrons produced. Then, there are many electron holes produced in the space charge region (SCR) or near the SCR, which is the sensitive volume of the transient effects. The electron holes produced in the sensitive volume are treated as the signals and then readout.

The target material is mainly Si or SiO_2, as used in sensitive volumes, integrated circuits, glass windows, etc., of the CIS. In order to analyze the interaction process between ^{60}Co gamma rays and the CIS, a cylindrical target detector in silicon or silicon oxide is established. The radius of the detector is 0.05 mm and the length is 0.1 mm. The 1.25-MeV gamma rays move straight from the left to the right through the center of the detector (as shown in Fig. 2a). The track, angle, and energy spectrum of produced electrons are simulated.

The structure of multilayer stack in a CIS pixel is shown in Fig. 2b. It is composed of a glass windows layer, passivation layer, silicon dioxide layer, interconnect layer, epitaxial layer, etc. There is 0.5 mm of air between the passivation layer and glass windows layer. The interconnect layers of the pixel were simplified as 3.7 μm aluminum (Al) layers and placed in the middle of SiO_2. A three-dimensional schematic of the gamma traversing through the 500 × 500-pixel CIS array for simulation is shown in Fig. 3. The 1.25-MeV gamma rays are incident randomly on the CIS array. The CIS array is defined and replicated by the CIS pixel. Then, the energy deposition of the gamma rays in the CIS array is simulated. The simulated image of the CIS under gamma ray radiation environments is calculated according to the energy deposition, which is simulated by Geant4 (as shown in Fig. 4).

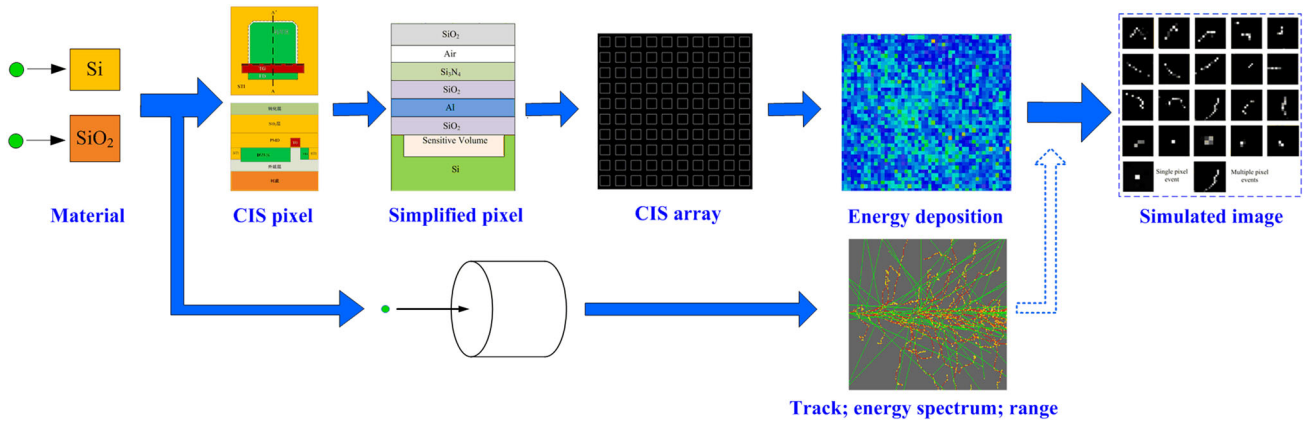

Fig. 1 (Color online) Schematic of global modeling project

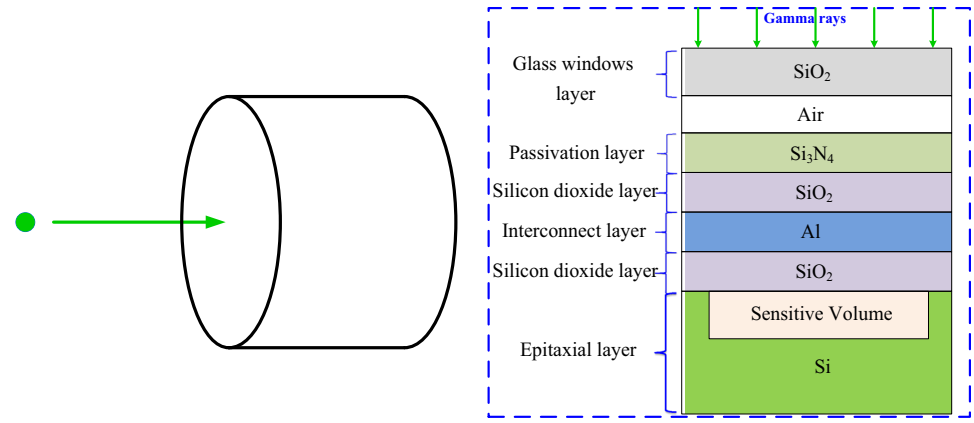

Fig. 2 Architecture of Geant4 simulation

(a) Cylindrical target detector **(b)** CIS pixel

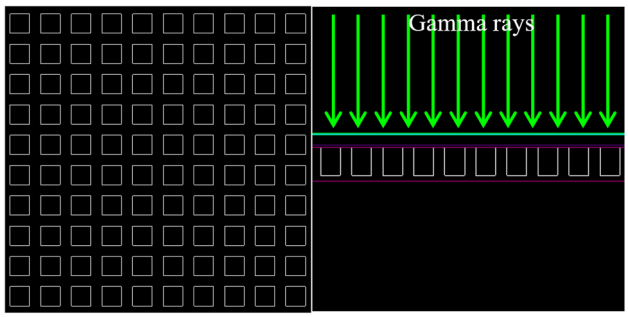

(a) Top view of the CIS array(regional enlarged) **(b)** Side view of the CIS array(regional enlarged)

Fig. 3 Diagram of the CIS array for simulation in Geant4

3 Experiment

The CIS contains a pixel array, a programmable gain amplifier (PGA) array, a low-power analog-to-digital amplifier (ADC) array, a serial periphery interface, and eight low-voltage differential signal (LVDS) channels. The full chip architecture of the CIS is shown in Fig. 5. The pixel array comprised 2048 × 2048 11-μm-pitch-4T-PPD pixels manufactured using a 0.18-μm CMOS process and front side illumination technology. The signals from the pixel array are amplified by PGA and then fed to the ADC for digitization. The digitized image signals are multiplexed and read out through eight LVDS outputs placed at the bottom of the chip.

The ^{60}Co gamma ray irradiation experiments were carried out in a laboratory at Northwest Institute of Nuclear Technology. The dose rate is approximately 0.1 rad(Si)/s, which is calibrated by the PTW UNIDOS [15] dosimetry system before irradiation. The dosimetry is accurate to closer than 2.5%. The system includes separate board, evaluation board, shielding box, computer control system, etc. The evaluation board and separate sensor board are separated and connected by a transmission circuit. There are no radiation-sensitive devices in the separate sensor board except the CIS. The evaluation board is placed into the shielding box to reduce the radiation damage on another device (for example, the FPGA). The evaluation board is controlled by a computer with evaluation software. The raw images are captured by the imaging system when the CIS is irradiated with ^{60}Co gamma rays.

4 Results and discussion

4.1 Simulation results

The transient effects of the gamma in the CIS are relevant to the electrons produced when the gamma traverses the CIS. The target material is mainly Si or SiO_2, as in CIS-sensitive volumes, integrated circuits, glass windows, etc. Therefore, the track of gamma rays and produced electrons when gamma rays traverse the Si or SiO_2 cube are simulated by Geant4, as shown in Fig. 6. The events are 2000 in our simulation works. From Fig. 6, we can see that when the gamma traverses the cube, there are many electrons (red lines in Fig. 6) around the path of incident gamma. In order to analyze the characteristic of the electrons, the

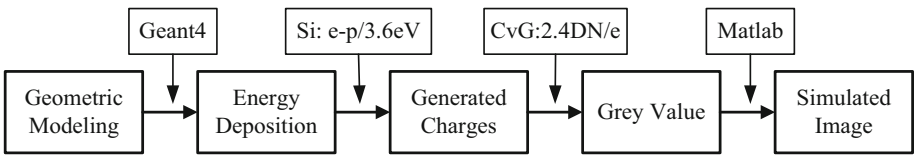

Fig. 4 Schematic diagram of the method to obtain the simulated image under gamma ray radiation environments

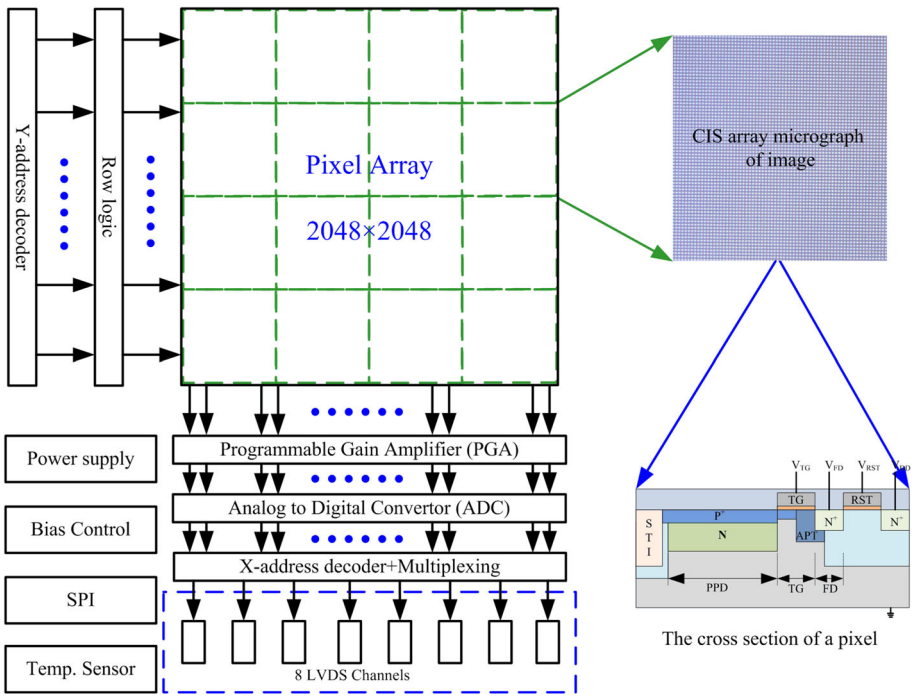

Fig. 5 (Color online) Full chip architecture of the CIS used in our irradiation experiments

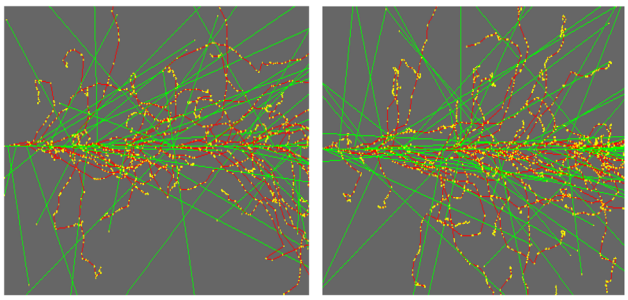

(a) Si **(b)** SiO_2

Fig. 6 (Color online) Example of 2000 simulation events in 0.1-mm Si and SiO_2 cubes

energy spectrum and angle of the electrons in Si and SiO_2 are calculated. Figure 7 gives the energy spectrum and angle of produced electrons in Si and SiO_2: (a) energy spectrum and (b) angle. From Fig. 7a, we can see that the energy of the produced electrons is in the range of 0 to 1 MeV. There are photoelectric effects, Compton scattering, and pair effects when the 1.25-MeV gamma ray traverses through the Si or SiO_2 cube, and the main effect is Compton scattering (for example, the cross section of the 1.25-MeV gamma ray in Si is approximately 2.659 barn, which is 99.89% of the total cross section). Therefore, there is a Compton plateau in the energy spectrum of the produced electrons. From Fig. 7b, we can see that the angle of the electrons ranges from 0° to 90°, which may lead to the electrons traversing through more than one sensitive volume of the pixel. Figure 8 gives the projected range of the electrons in Si and SiO_2. From Fig. 8, we can see that the project range of the electrons is near 1000 μm in Si or SiO_2 when the energy is approximately 1 MeV. The pixel size of the CIS is approximately 11 μm. Therefore, the electrons may pass through tens of pixels of the CIS array, which may be observed in the output images of the CIS. From Figs. 6, 7, and 8, there is no obvious difference between the gamma traversing through Si or SiO_2. Therefore, to simplify the simulation structure of the CIS array, Si is used to replace SiO_2 of shallow trench isolation material in our simulation.

As described in Sect. 2, the electrons mainly produced by photoelectric effects, Compton scattering, or pair effects would interact with the pixels of the CIS and generate electron holes on a cluster of pixels, which would be detected as an illuminated region on the read images captured in complete darkness. Figure 9 shows the simulated image of the CIS induced by gamma rays. The 100 × 100 pixel image, which is regionally enlarged to a 500 × 500 pixel image, is shown in Fig. 9a. The detected events can be divided into two types: single pixel event and multiple pixel events (as shown in Fig. 9b), which is similar to the events in a charge-coupled device under radiation environments [16].

A single pixel event means that only one pixel has collected the electron holes. A multiple pixel event means that more than one adjacent pixel has collected the electron holes. The multiple pixel events could be a two-branch, a straight line, a curve, or a spot-shaped form. The two-branch shaped form of multiple pixel events may be induced by the electrons generated in pair effects. The

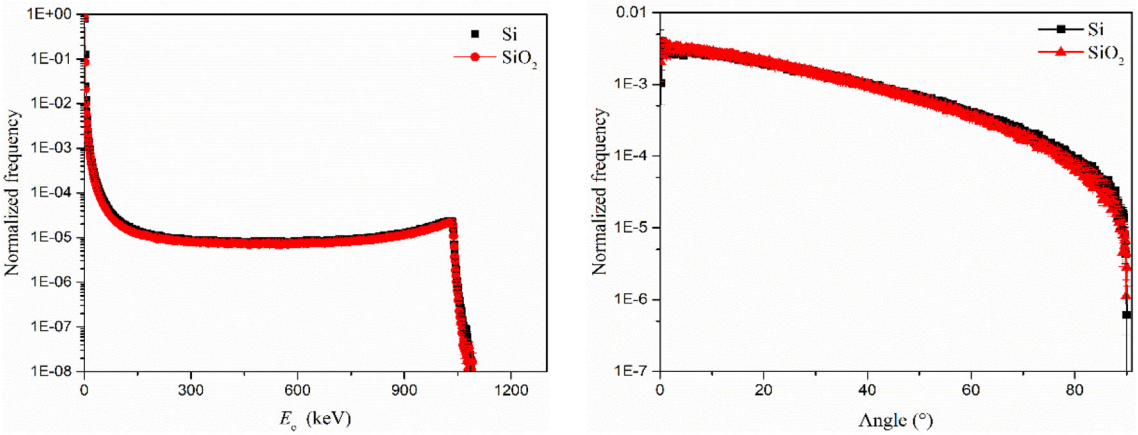

(a) Energy spectrum (b) Angle

Fig. 7 (Color online) Energy spectrum and angle of produced electrons in Si and SiO_2

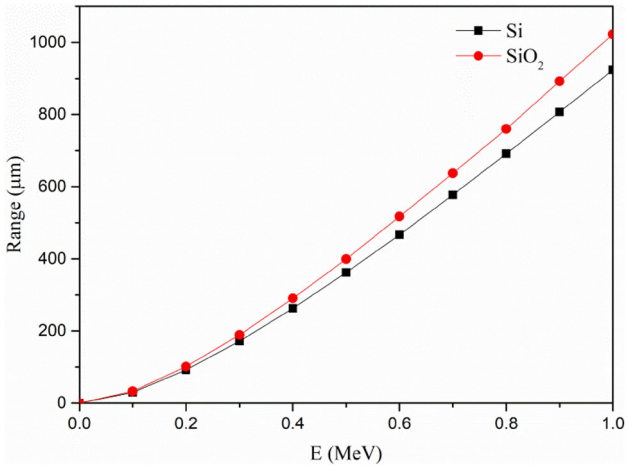

Fig. 8 Projected range of the electrons in Si and SiO_2

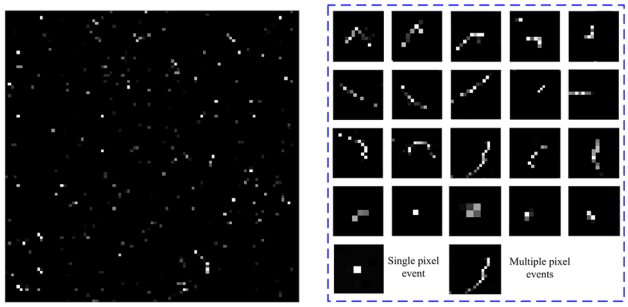

(a) 100×100 pixel simulated image (b) Typical pixels events

Fig. 9 Simulated image of the CIS induced by gamma

straight line or curve-shaped form of multiple pixel events is induced by electrons generated in photoelectric effects, Compton scattering, or pair effects.

4.2 Experimental results

Figure 10a shows the experimental 100 × 100 pixel image of the CIS induced by gamma rays. From Fig. 10a, we can see that the single pixel event and multiple pixel events are observed in the output image under completely dark environments. The two-branch, straight line, curve, and spot shape are also included in the multiple pixel events, as shown in Fig. 10b. Figure 11 gives a comparison between typical simulation and experimental pixels events: Fig. 11a–c are simulation results; Fig. 11d–f are experimental results. From Fig. 11, one can see that the shape of the simulated multiple pixel events looks the same as the experimental results. However, the track widths of the experimental results are bigger than those of the simulation results. The track width of the simulation is approximately one pixel, but the track width in the experiment is more than two pixels. This is mainly because the electron holes collected in SCR of the pixel reach full well charges, and the charges may spread to neighboring or adjacent pixels by diffusion, which is known to cause crosstalk, and expand the track width.

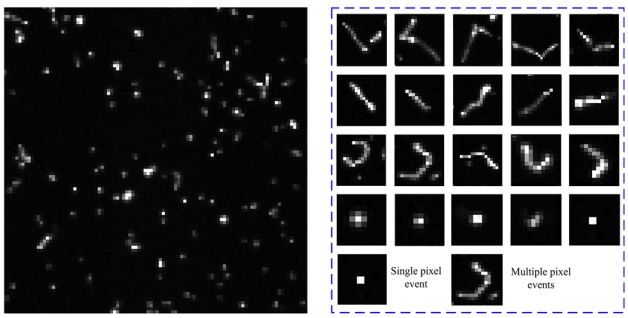

(a) 100×100 pixel experimental image (b) Typical pixel events

Fig. 10 Experimental image of the CIS induced by gamma

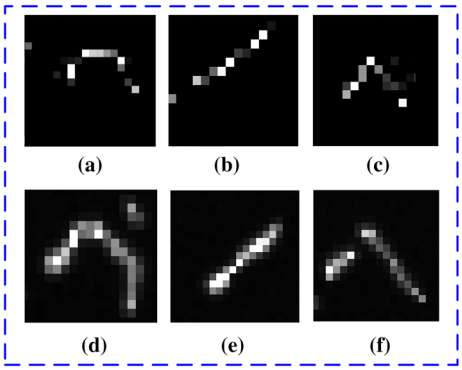

Fig. 11 Comparison between typical simulation and experimental pixel events: **a–c** are simulation results; **d–f** are experimental results

4.3 Discussion

The electron holes near the SCR could diffuse in the SCR and then become readout. Therefore, the exact dimension of the sensitive volume, which includes both SCR and the region near the SCR, is difficult to obtain. However, it is important to simulate the results. Figure 12 gives the number of the good events (data points) versus the height of the sensitive volume (with 28,000,000 events simulated). A good event is an event in which electron holes are generated in more than one pixel. The number of such events corresponds to the number of multiple pixel events. From Fig. 12, we can see that the height of the sensitive volume has a significant effect on the transient effects. When the height of the sensitive volume is approximately 2 μm, there are approximately 2759 good events, but when the height of the sensitive volume is approximately 10 μm, there are almost 30000 good events. The number of good events increases rapidly with increasing height of the sensitive volume, and the goodness

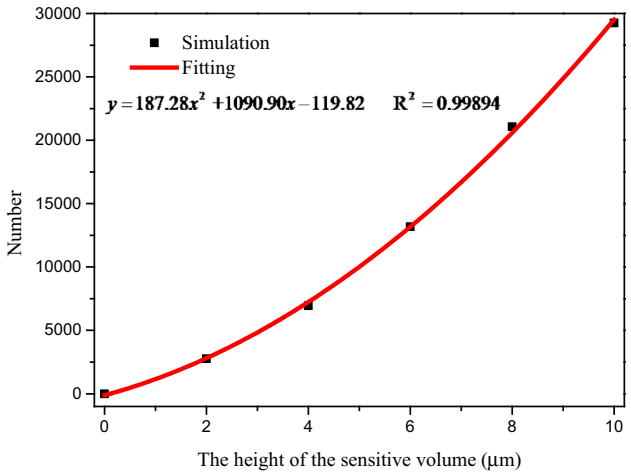

Fig. 12 Number of the good events versus the height of the sensitive volume

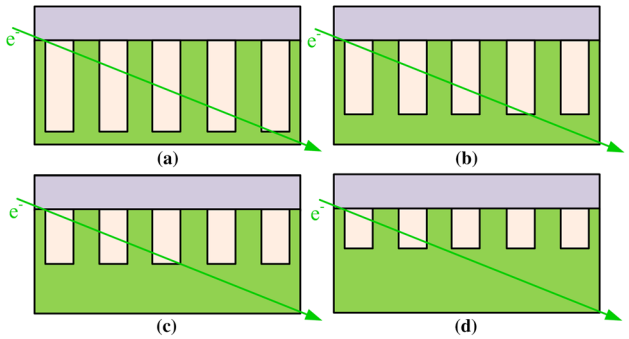

Fig. 13 Schematic diagram of an electron traversing through the CIS array with different sensitive volume heights

of fit of the binomial fitting is $R^2 = 0.99894$. Figure 13 shows a schematic diagram of the electron traversing through the CIS array with different sensitive volume heights. From Fig. 13, we can clearly see that the larger the height of the sensitive volume is, the more pixels an electron traverses through. Therefore, the good events increase with increasing height of the sensitive volume.

Besides, when the gamma rays transfer through the glass window that covers the CIS, there are many produced electrons, which may have some effects on the output signals of the CIS imaging system in a gamma ray radiation environment. In addition, the pixel size, energy, and exposure angle of the metal interconnect overlayers may also have effects on the output signals of the CIS imaging system. More experiments should be carried out in consideration of this.

5 Conclusion

In this study, the transient effects of ^{60}Co gamma rays in CIS were modeled using the Monte Carlo method based on Geant4. The track, energy spectrum, and angle of produced electrons of 1.25 MeV gammas in Si and SiO_2 were calculated, which can help us to understand the transient effects of ^{60}Co gamma rays in CISs. The transient effects of 1.25 MeV gammas in a 500 × 500 CIS array were simulated. The simulation results and experimental results were compared.

The detected events of the transient effects of ^{60}Co gamma rays in the CIS could be divided into two types: single pixel event and multiple pixel events. The multiple pixel events could have two-branch, straight line, curve, or spot-shaped form. The shapes in the experiment and simulation are similar to each other, except the width of the track, which may be induced by crosstalk. In addition, the sensitive volume height has great effects on the transient effects. More experiments and simulation works should be carried out in consideration of this.

References

1. V. Goiffon, M. Estribeau, P. Magnan, Overview of ionizing radiation effects in image sensors fabricated in a deep-submicrometer CMOS imaging technology. IEEE Trans. Electron Dev. **56**, 2594–2601 (2009). https://doi.org/10.1109/ted.2009.2030623
2. F. Wang, M.Y. Wang, Y.F. Liu et al., Obtaining low energy γ dose with CMOS sensors. Nucl. Sci. Tech. **25**, 060401 (2014). https://doi.org/10.13538/j.1001-8042/nst.25.060401
3. G.R. Hopkinson, Radiation effects in a CMOS active pixel sensor. IEEE Trans. Nucl. Sci. **47**, 2480–2485 (2002). https://doi.org/10.1109/23.903796
4. G.R. Hopkinson, A. Mohammadzadeh, R. Harboe-Sorensen, Radiation effects on a radiation tolerant CMOS active pixel sensor. IEEE Trans. Nucl. Sci. **51**, 2753–2762 (2004). https://doi.org/10.1109/TNS.2004.835108
5. V. Goiffon, P. Magnan, O. Saint-Pé et al., Ionization versus displacement damage effects in proton irradiated CMOS sensors manufactured in deep submicron process. Nucl. Instrum. Methods A **610**, 225–229 (2009). https://doi.org/10.1016/j.nima.2009.05.078
6. V. Goiffon, M. Estribeau, P. Cervantes et al., Influence of transfer gate design and bias on the radiation hardness of pinned photodiode CMOS image sensors. IEEE Trans. Nucl. Sci. **61**, 3290–3301 (2014). https://doi.org/10.1109/TNS.2014.2360773
7. C. Virmontois, C. Durnez, M. Estribeau et al., Radiation effects in pinned photodiode CMOS image sensors: variation of epitaxial layer thickness. IEEE Trans. Nucl. Sci. **64**, 38–44 (2016). https://doi.org/10.1109/TNS.2016.2641162
8. Z.J. Wang, W.Y. Ma, J. Liu et al., Degradation and annealing studies on gamma rays irradiated cots ppd CISs at different dose rates. Nucl. Instrum. Methods A **820**, 89–94 (2016). https://doi.org/10.1016/j.nima.2016.03.006
9. Y.Y. Xue, Z.J. Wang, W. Chen et al., Modeling dark signal of CMOS image sensors irradiated by reactor neutron using Monte Carlo method. Sci. China (Inf. Sci.) **6**, 062405 (2018). https://doi.org/10.1007/s11432-017-9323-0
10. Y.Y. Xue, Z.J. Wang, M.B. Liu et al., Research on proton radiation effects on CMOS image sensors with experimental and particle transport simulation methods. Sci. China (Inf. Sci.) **60**, 120402 (2017). https://doi.org/10.1007/s11432-017-9250-7
11. Q.Q. Cheng, Y.Z. Yuan, C.W. Ma et al., Gamma measurement based on CMOS sensor and ARM microcontroller. Nucl. Sci. Tech. **28**, 122 (2017). https://doi.org/10.1007/s41365-017-0276-x
12. S. Agostinelli, J. Allision, K. Amako et al., Geant4—a simulation toolkit. Nucl. Instrum. Methods A **506**, 250–303 (2003). https://doi.org/10.1016/S0168-9002(03)01368-8
13. J. Allison, K. Amako, J. Apostolakis et al., Geant4 developments and applications. IEEE Trans. Nucl. Sci. **53**, 270–278 (2006). https://doi.org/10.1109/tns.2006.869826
14. C. Amsler, M. Doser, M. Antonelli et al., Review of particle physics. Phys. Lett. B **667**, 1–6 (2008). https://doi.org/10.1016/j.physletb.2008.07.018
15. W. Arshed, K. Mahmood, I. Qazi et al., A comparison of in-air and in-water calibration of a dosimetry system used for radiation dose assessment in cancer therapy. Nucl. Technol. Radiat. Prot. **25**, 51–54 (2010). https://doi.org/10.2298/NTRP1001051a
16. T.S. Saoud, S. Moindjie, J.L. Autran et al., Use of CCD to detect terrestrial cosmic rays at ground level: altitude vs. underground experiments, modeling and numerical Monte Carlo simulation. IEEE Trans. Nucl. Sci. **61**, 3380–3388 (2014). https://doi.org/10.1109/tns.2014.2365038